Catalysis Letters Vol. 100, Nos. 1–2, March 2005 (© 2005)
DOI: 10.1007/s10562-004-3096-7

Strong dependence on pressure of the performance of a Co/SiO_2 catalyst in Fischer–Tropsch slurry reactor synthesis

V.A. de la Peña O'Shea, M.C. Alvarez-Galvan, J.M. Campos-Martin, and J.L.G. Fierro*

Instituto de Catálisis y Petroleoquímica, CSIC, c/Marie Curie, s/n, Cantoblanco, 28049 Madrid, Spain

Received 30 September 2004; accepted 09 November 2004

A 10 wt% Co/SiO_2 catalyst was prepared by the incipient wet-impregnation method and tested in Fischer–Tropsch synthesis in a slurry reactor under conditions approaching industrial practice. The catalyst precursor was investigated by X-ray diffraction (XRD), temperature-programmed reduction (TPR), transmission electron microscopy (TEM) and photoelectron spectroscopy (XPS). The XPS and XRD techniques revealed the presence of a crystalline Co_3O_4 spinel-type phase, while-in addition-TEM and XPS analyses pointed to the formation of another amorphous Co_3O_4 spinel phase, both species interacting weakly with the silica substrate. The influence of total pressure on the conversion, selectivity and stability of the catalyst was studied. Upon increasing the overall pressure from 20 to 40 bar, not only activity increased but also the catalyst are not deactivating. These results are explained in terms of an increase of gases solubility in the solvent, this increment of CO concentration in the liquid phase favours carbonyl species formation and the cobalt particles segregation that implies an increase in the metal surface area.

KEY WORDS: FT synthesis, cobalt catalyst, pressure effect, slurry reactor.

Introduction

Supported cobalt catalysts have been successfully applied in the Fischer–Tropsch synthesis (FTS) of high-molecular weight paraffin waxes, which can be hydrocracked to produce lubricants and clean diesel fuels. One important issue in the development of this process is the improvement of catalyst activity by increasing the number of active metal sites that are stable under the prevailing reaction conditions. The production of liquid hydrocarbons over cobalt catalysts was first reported in 1913 in a patent granted by BASF [1]. Over the ensuing nine decades, different groups have reported the performance of supported cobalt catalysts, studying the effect of promoters [2–6], and support [7–9] and preparation [10,15] methods. The formation of active species on the surface of a cobalt-based catalyst depends on several processing parameters, such as the method of impregnation employed, and the temperature and calcination time. It has been reported that hydrocarbon formation in FTS is not only dependent on the support or on the degree of cobalt dispersion, but is also very much dependent on the number and availability of active sites present in the catalyst system [11,16].

It has been suggested that, on cobalt catalyst, FTS is a structural-insensitive reaction and the active phase is the cobalt metal. Therefore, cobalt catalysts with high reduction degree and high cobalt dispersion show high activity for FTS, and the Co catalyst activity may be predicted directly from cobalt dispersion values of reduced catalyst measured by hydrogen chemisorptions [16–18].

However, structural changes of cobalt catalysts during FTS may result in a variation in the number of the active sites, so that the catalyst shows a change in the activity of FTS than the predicted values. Therefore, investigations on structural changes during FTS synthesis are meaningful for further understanding of the catalytic property–structure relationship, and are helpful for developing cobalt FTS catalyst. The structural changes during performing FTS may include the transformation of the metallic cobalt species to cobalt carbides and/or cobalt oxides and the aggregation or segregation of the metallic cobalt particles. Nowadays it is widely accepted that cobalt has a lower tendency to produce carbides than Fe and remain in metallic state [19,20]. Recently, the selforganisation of metal particles occurs under FTS conditions with cobalt catalyst. Bian *et al.* [21] observed an aggregation of the Co^0 crystallites, while Schulz *et al.* [22] observed a reconstruction of the cobalt crystallites producing a segregation of theses particles. Nickel surface segregation by CO adsorption has been reported by Ponec *et al.* [23]. Images of cobalt surfaces (surface segregation) by FTS has been published by Wilson *et al.* [24]. De la Peña *et al.* [25] in recent studies of the influence of the pretreatment in the FTS observed an amount of the activity when the cobalt catalyst are activated in syngas atmosphere, being due this behaviour to a segregation of the cobalt crystallites in the catalyst.

The main technical problems of FT synthesis include the need for rapid removal of the reaction heat, which

---

*To whom correspondence should be addressed.
E-mail: jlgfierro@icp.csic.es

amounts to about 25% of the heat of combustion of the synthesis gas. Thus, local overheating of the catalyst favours methane formation. The use of a stirred tank reactor avoids local hot spots on the catalyst surface and favours heat withdrawal. Notwithstanding, in batch reactors both the pretreatment and reaction conditions appear to be very critical for obtaining good catalyst performance.

The aim of the present work is the study of the pressure effect in the possible morphological changes produced in a cobalt system during FTS. A Co/SiO$_2$ catalyst was prepared by impregnation method whit cobalt nitrate and calcinated in O$_2$ atmosphere during 2 h. The election of this system is due than in this case the interaction between support and the metallic phase is low [26] and the effect of the pressure under reactions conditions only affect to the active phase.

Experimental

Catalyst preparation

The silica-supported cobalt (10% Co) catalyst was prepared by the incipient wet-impregnation of a Grace Division silica carrier (319 m^2/g, 1.22 cm^3/g) with an aqueous solution of cobalt nitrate hexahydrate ([Co(NO$_3$)$_2$] · 6H$_2$O, Merck reagent grade). The impregnate was dried in air at 393 K for 12 h, and then calcined in flowing air at 773 K for 2 h. The catalyst is labelled Co10-c.

Characterization techniques

The cobalt content of the catalyst was determined by the inductively coupled plasma (ICP) technique using a Perkin–Elmer Optima 3300 DV device. Specific areas were calculated using the BET method from the nitrogen adsorption isotherms, recorded at the temperature of liquid nitrogen using a Micromeritics apparatus, model ASAP–2000, taking a value of 0.162 nm^2 for the cross-sectional area of the N$_2$ molecule adsorbed at 77 K. Prior to adsorption measurements, samples were outgassed at 423 K.

Powder X-ray diffraction (XRD) patterns of the precursor and calcined samples were recorded using a Seifert 3000 P diffractometer, using nickel-filtered Cu K$_{\alpha1}$ ($\lambda = 0.15406$ nm) radiation. Step scan of 0.02° was taken between 5° and 80° Bragg angle.

Temperature-programmed reduction (TPR) experiments were carried out with a Micromeritics TPD/TPR 2900 apparatus equipped with a thermal conductivity detector. Reduction profiles were obtained by passing a 10% H$_2$/Ar flow at a rate of 50 mL(STP) min^{-1} through the sample (weight around 30 mg). Temperature was increased from 300 to 1273 K at a rate of 10 K min^{-1}, and the amount of hydrogen consumed was determined as a function of temperature. Under these conditions, the line profile and peak position can be measured accurately.

Transmission electron micrographs were taken with a Fei Tecnai G30. The acceleration voltage was set at 200 kV. The powdered sample was first suspended in acetone, after which a drop of the suspension was deposited on a copper grid covered by a fine carbon membrane evaporated under vacuum.

X-Ray photoelectron spectra (XPS) were acquired with a VG Escalab 200R spectrometer equipped with a hemispherical electron analyzer and an AlK$_{\alpha1}$ ($h\nu$ = 1486.6 eV, 1 eV = 1.6302×10^{-19} J) X-ray source. The powdered samples were mounted on a sample rod placed in a pretreatment chamber and degassed for 1 h. Once the sample had been analysed, it was replaced in the pretreatment chamber and reduced *in situ* under H$_2$ at 773 K. The quantification procedure has been reported elsewhere [27]. All binding energies (BE) are referred to the C 1s line at 284.9 eV. This reference gives accurate (±1 eV) binding energy values.

Catalytic activity

Activity tests were carried out using an autoclave high pressure (Autoclave Engineers, Ltd.) catalytic reactor. The catalysts (0.5 g) were activated in a mixture of N$_2$/H$_2$ = 8:2 at 773 K for 10 h under atmospheric pressure. The reaction was conducted at 503 K and different pressures: 2, 3, 3.5 and 4 MPa. The composition of the feed stream – CO (30%), H$_2$ (60%) and N$_2$ (10%) – was adjusted by electronic mass flow controllers (Brooks) to a total flow of 100 mL(STP) min^{-1}. The reactor was suitably designed in order to allow on-line analysis of the gas fraction through a multiple GC column system. A Hewlett Packard 6890 gas chromatograph equipped with an HP-1 capillary column and a Haysep Q packed column were used for product separation on-line. Product analysis was carried out with thermal conductivity (TCD) and flame ionisation (FID) detectors, which allows the analysis of H$_2$, CO, CO$_2$, C$_1$–C$_6$ hydrocarbons. C$_7$–C$_{30}$ hydrocarbons were analysed in a Hewlett Packard 5890 gas chromatograph equipped with an HP-1 column.

Results and discussion

Catalyst texture

The nitrogen adsorption–desorption isotherms of the silica substrate and catalyst belong to type IV of the IUPAC classification, and exhibit a hysteresis loop (H1) located at relatively high pressures of the absorbent, typical of porous materials or compact packing of nearly uniform regularly ordered microspheres [28]. The BET area and pore volume of calcined SiO$_2$ were S_{BET} = 299 m^2/g, and $V_{\mathrm{p}=1.2}$ cm^3/g, which were markedly decreased upon cobalt incorporation (Co10-c sample: $S_{\mathrm{BET}=219}$ m^2/g and $V_{\mathrm{p}=0.8}$ cm^3/g). However, average pore diameter, as determined by the BJH method to the desorption branch of the isotherm, was almost constant: about 10 nm.

Crystalline phases

The XRD pattern recorded for the calcined Co10-c catalyst only exhibited diffraction lines of Co_3O_4 oxide (JCPDS 78-1970). Nevertheless, from the X-ray diffraction measurements alone amorphous or highly dispersed Co-containing phases cannot be detected. The size of Co_3O_4 crystallites was calculated using the Debye–Scherrer equation. A value of 21.0 nm was obtained for the crystal size of the Co_3O_4 crystallites. This clearly indicates that the dispersion of cobalt species was low. XRD pattern of the catalyst reduced in an H_2 atmosphere at 773 K displayed diffraction lines of metallic Co^0 (JCPSD 1-1255). The particle size of the metallic Co^0 particles, estimated by the Debye–Scherrer equation, was 17.0 nm, which is comparable to that obtained for Co_3O_4 crystallites present in the calcined catalyst precursor. Thus, it appears that no sintering of the metal particles occurs along the reduction step.

TEM analysis revealed that cobalt species were not homogeneously distributed in the silica support. Nearly spherical aggregates of Co_3O_4 particles were deposited inside the pores of the support and also on its external surface. These aggregates were of different sizes, some particles being of a size comparable to that determined by XRD, although a few aggregates were larger (200–1200 nm). These latter aggregates were preferentially located near the external silica surface. Activated sample in H_2 does not show substantial structural differences with respect the unreduced counterpart.

The TPR profile obtained for a Co_3O_4 sample and the Co10-c precursor is shown in figure 1. The reduction profile of this precursor shows two reduction peaks, similar to those observed in bulk Co_3O_4 oxide. The first one – of low intensity – starts at approximately 475 K and overlaps the more intense one, whose maximum is located at about 596 K. Depending on the experimental conditions, the reduction of the Co_3O_4 bulk proceeds in two steps: the first involves the reduction of Co^{3+} ions present within the spinel structure to Co^{2+} (equation (1)), with the subsequent structural change to CoO, followed by the reduction of CoO to metallic cobalt (equation (2)) [29–31].

$$Co_3O_4 + H_2 \rightarrow 3CoO + H_2O \quad (1)$$

$$3CoO + 3H_2 \rightarrow 3CO^0 + 3H_2O \quad (2)$$

The TPR profile depends on the dispersion of the supported metal oxide and on the interaction between the support and the active phase. This profile was compared with that of a bulk Co_3O_4 sample. The shape of the TPR profile of bulk Co_3O_4 was essentially the same as that of the supported Co10-c catalyst precursor, although it appeared shifted to higher temperatures. The shift in the reduction profile of bulk Co_3O_4 towards higher temperature must be related to particle-size effects.

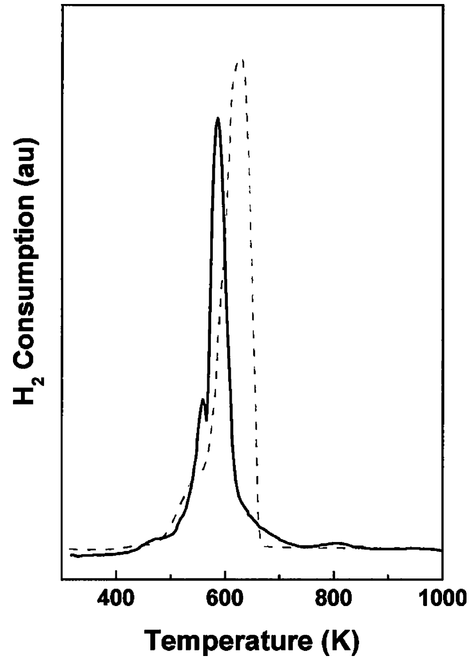

Figure 1. TPR profile of the Co10-c catalyst (solid line) and Co_3O_4 (dash line).

The chemical state of the elements and their relative abundances on the catalyst surface were explored using photoelectron spectroscopy. The binding energies of core Co 2p and Si 2p core-levels were measured. Fitting the Co 2p peaks of the Co10-c sample revealed two contributions: one at 779.9 eV, associated with Co^{3+} (octahedral), and another at 782.3 eV, corresponding to Co^{2+} (tetrahedral). In addition, the characteristic satellite line of Co^{2+} ions located at high binding energies was also observed. These values are in good agreement with those reported in the literature [20,32]. The surface atomic ratio between Co^{3+} and Co^{2+} is close to 2 and corresponds to the $Co^{2+}(Co^{3+})_2O_4$ spinel-type mixed oxide phase. The atomic ratio of the surface species (Co2p/Si2p) is 0.01. This low value indicates that cobalt oxide dispersion was very low, in agreement with the XRD and TEM observations. In short, XPS and XRD techniques showed the presence of Co_3O_4 spinel-type phase.

The photoelectron spectrum of the Co10-c sample reduced in an H_2 atmosphere at 773 K was different from that of the calcined counterpart. Three contributions, instead of two, could be distinguished in the most intense Co $2p_{3/2}$ emission: one peak at 779.7 eV was assigned to octahedral Co^{3+} ions, probably arising from the unreduced Co_3O_4 phase; another peak at a 782.0 eV, attributed to Co^{2+} (octahedral) for CoO, and a third peak at a BE of 777.7 eV, associated with metallic Co^0. Moreover, the intensity of the satellite line of the $Co2p_{3/2}$ peak for the reduced sample increased with respect to the, calcined counterpart, which is indicative of an increase in the proportion of Co^{2+} species in the reduced sample. These results suggest that the reduction of Co_3O_4 proceeds in two steps but – also – that the second step starts before the reduction of the Co_3O_4 to CoO has been completed.

The XPS analysis of the samples used in reaction were performed but the results for the cobalt species are very poor, because all samples become covered by heavy hydrocarbons and/or coke deposits that block the active sites than made impossible this study.

The behaviour of the Co10-c catalyst in the FT synthesis was examined. The degree of CO conversion as a function of the reaction time for pressure levels ranging from 2 to 4 MPa is shown in figure 2. An increase in pressure led to a higher CO conversion level [33]. The higher reaction rate, induced by pressure, may be due to an increase in the solubility of both CO and H_2 in the solvent when the overall pressure is increased [34].

On the other hand, the catalyst became completely deactivated for reaction times no longer than 6–8 h under the lower pressures (2–3 MPa). At pressures of 3.5 MPa and above, the reaction rate increased markedly, CO conversion: 20% at 3.5 MPa and 30% at 4 MPa. Besides, the catalyst deactivation was clearly diminished during the reaction time studied, operating at higher pressures.

The principal reason of the low activity and deactivation of the cobalt catalyst in the FTS is the large size of the cobalt particles, and Co catalyst whit high cobalt dispersion shows a high activity and stability in FTS [16,17]. The characterization data, especially TEM images showed a very high particle size, that implies a low dispersion. This fact explains the low conversion and the deactivation of the cobalt catalyst to pressures of 2 and 3 MPa. Nevertheless, an increase in the overall pressure to 3.5 or 4 MPa produce an increase in the H_2 and CO solubility, which have a great influence in the catalyst behaviour. Firstly, an increase of H_2 concentration in the liquid phase inhibits the surface oxidation due to water presence in the reaction medium. As second effect, an increase in the carbon monoxide concentration in the liquid phase could produce a reorganization of the metal particles, taking place a dispersion and segregation of the active phase. This second effect was confirmed by XRD used catalyst (figure 3). The XRD patterns were different for the catalyst used under different reaction conditions. Catalyst used at 2 MPa showed a peak attributed to the metallic species together with CoO lines (JCPDS 9-402), which is a clear indication of the partial oxidation of the metallic phase, probably for the water presence in the reactor. XRD of catalyst used at 3 MPa only exhibit the diffraction lines of Co^0. However, for the catalysts used at higher pressures (3.5 and 4 MPa) no diffraction peak of cobalt species were detected. This finding was consistent with TEM analysis of samples exposed to a H_2 + CO mixture, in which, the cobalt particles appear much more dispersed on the silica substrate than the activated with only hydrogen. These facts would indicate a reorganization of the metal particles morphology, which probably gives to a segregation of the cobalt particles, through CO chemisorption, producing a disproportionation of plane sites in site of low coordination on top positions and sites of high coordination in a vacant position, which produce a modification in activity and selectivity.

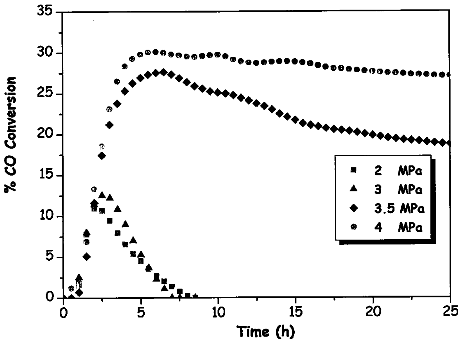

Figure 2. Evolution of CO conversion with the reaction time at several different pressures on the Co10-c catalyst.

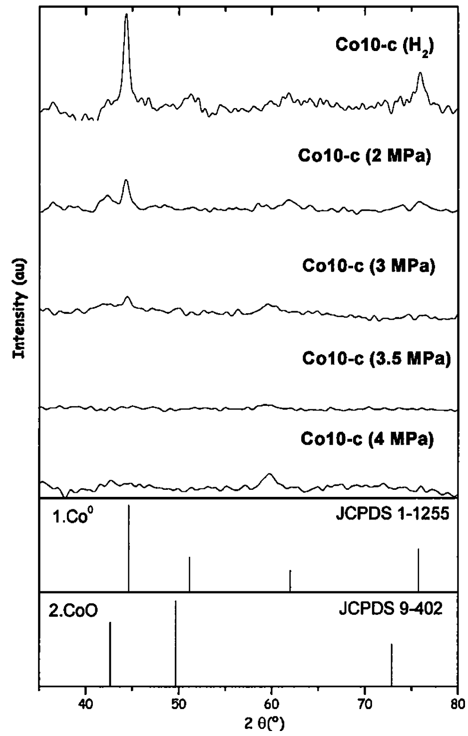

Figure 3. DRX profiles of the different catalyst after reduction and after reaction.

This catalyst reconstruction is attributed to the strong CO chemisorption on cobalt [35] that allows (thermodynamically) carbonyl formation during FTS. Then the reaction of CO with metal surface can be assumed to induce surface reconstructing in direction to surface enlargement through segregation. Segregation of the surface will be favoured against sintering if the free energy of CO adsorption overcompensates that of reducing the surface area through sintering. Surface segregation can explain the observed increase in activity and stability with higher pressures, as segregation means an increase of the specific surface area and, respectively, of the number of the active sites.

Finally, the overall, pressure also led to some changes in product selectivity (table 1). The product distribution at 2 MPa showed high selectivity for methane and light hydrocarbons, and light production of C_{6+} products. A change in selectivity occurs for reactions with operation pressures above 3 MPa, which include a decrease in selectivity towards methane and light hydrocarbons and a consequent increase in the higher hydrocarbons selectivity, this increment was more pronounced at higher pressures. These results are coherent with the increase of the CO conversion, which favours the chain growing due to the increase of the active sites number of due to metallic segregation. In relation to carbon dioxide, this is not observed for reaction conducted at 2 MPa, being its formation very low for reactions pressures above 2 MPa.

It was been observed Schulz *et al.* [22] that the surface segregation through strong CO chemisorption produces a large increase of the number of sites and the sites disproportionate into sites of higher and lower coordinations on the expense of plane site. The on top sites of low coordination allow reactions of chain growth, due to the existence in these peak and mountain sites of several free valence for binding surface species and ligands. The sites of high coordination (in holes and valleys) preferentially give CO dissociation. The common hydrogenation sites (plane sites) would be seriously poisoned, through strong CO chemisorption. This fact would explain the product distribution obtained in our work, in which the increase of the proportion of C_{6+} hydrocarbon (and the decrease of light hydrocarbon) whit pressure increase would be ought to cobalt particles segregation.

Table 1

Influence of pressure on the activity and selectivity[a] of the Co10-c catalyst

Pressure (MPa)	%CO Conversion	C_1	C_2	C_3	C_4	C_5	C_{6+}	CO_2
2	11	32	6	10	9	7	36	–
3	13	22	4	8	7	5	53	2
3.5	28	18	3	7	5	4	60	3
4	31	22	3	5	4	2	62	2

Experimental conditions: $T = 503$ K, H_2/CO = 2/1, total flow = 100 mL/min (maximum values).

[a] Selectivity = mol CO to product/mol CO total consumed.

Conclusions

The main conclusions that can be drawn from this study are as follows: (i), the Co10-c catalyst prepared by the incipient wet-impregnation method developed two kinds of Co_3O_4 species: a crystalline phase with a crystal size of 21.0 nm, and another amorphous phase of larger particle size (>200 nm). (ii), the interaction of Co_3O_4 particles with the support surface is very weak, as may be inferred from the similarity of the TPR profiles of the Co10-sample and a bulk Co_3O_4 reference sample. (iii) under the reaction conditions and an operation pressure lower than 3 MPa, large cobalt particles rapidly become are deactivated due to poisoning by strong CO chemisorption; only at pressures of around 4 MPa the catalyst surface maintain stable activity as a consequence of the improved solubility of CO and H_2 in the solvent and therefore the greater CO adsorption. This fact produces a segregation of the cobalt particles increasing of the specific surface area and, respectively, of the number of the active sites. This is traduced in a higher of the CO conversion. This segregation also produces changes in the product selectivity, decreasing the selectivity towards methane and light hydrocarbon (lower than C_6) and increasing the selectivity towards C_{6+} hydrocarbons. The modification in the product distribution is explained in relation to a catalyst active sites restructuring processing, in which the sites are disproportionate into sites of lower and the higher coordination. The lower ones will promote alkyl growth reactions and the higher ones will favour CO dissociation.

Acknowledgments

A fellowship (VPO) granted by the Repsol-YPF Foundation is acknowledged. JMCM acknowledges financial support from the Ministerio de Ciencia y Tecnología (Spain) in the Ramon y Cajal Program. This work was partly supported by MCYT (Spain) (Project MAT2001-2215-C03-01).

References

[1] German Patent 293,787, Process for production of Hydrocarbons and their derivatives, assigned to BASF, granted March 8, 1913.

[2] G. Jacobs, T.K. Das, Y. Zhang, J. Li, G. Racoillet and B.H. Davissd, Appl. Catal. A: Gen. 233 (2002) 263.

[3] J. Panpranot, J.G Goodwin Jr. and A. Sayari, J. Catal. 211 (2002) 530.

[4] S. Sun, K. Fujimoto, Y. Yoneyama and N. Tsubaki, Fuel 81 (2002) 1583.

[5] G.W. Huber and C.H. Bartholomew, Stud. Surf. Sci. Catal. 136 (2001) 283.

[6] S. Ali, B. Chen and J.G. Goodwin, J. Catal. 157 (1995) 35.
[7] R.L. Chin and D.M. Hercules, J. Phys. Chem. 86 (1982) 360.
[8] H.M. Bruce and G. Baker, Appl. Catal. A: Gen. 123 (1995) 23.
[9] E. Coulter Kent and A.G. Sault., J. Catal. 154 (1995) 56.
[10] S. Sun, L. Fan and K. Fujimoto Chem. Lett. (1999) 343.
[11] E. Iglesia, S.C. Reyes, R.J. Madon and S.T. Soled, Adv. Catal. 39 (1993) 221.
[12] E. Iglesia, S.L. Soled, R.A. Fiato and G.H.A. Via, J. Catal. 143 (1993) 345.
[13] R.C. Reuel and C.H. Bartholomew, J. Catal. 85 (1985) 63.
[14] R.C. Reuel and C.H. Bartholomew, J. Catal. 85 (1985) 78.
[15] B.A. Sexton, A.E. Hughes and T.W. Turney, J. Catal. 97 (1986) 390.
[16] B.G. Johnson, C.H. Bartholomew and D.W. Goodman, J. Catal. 118 (1991) 231.
[17] E. Iglesia, Appl. Catal. A 161 (1997) 59.
[18] N. Tsubaki, S. Sun and K. Fujimoto, J. Catal. 199 (2001) 236.
[19] B. Ernst, A. Bensaddik, L. Hilarie, P. Chaumette and A. Kiennemann, Catal. Today 39 (1998) 329.
[20] B. Ernst, A. Bensaddik, L. Hilarie, P. Chaumette and A. Kiennemann, Appl. Catal. A 186 (1999) 145.
[21] G. Bian, N. Fujishita, T. Mochizuki, W. Ning and M. Yamada, Appl. Catal. A 252 (2003) 251.
[22] H. Schuluz, Z. Nie and F. Ousmanov, Catal Today 71 (2002) 351.
[23] V. Ponec, W.L. Dijk and J.A. Groenewegen, J. Catal. 45 (1976) 277.
[24] J.H. Wilson and G.P.M. Groot, J. Chem. Phys. 99 (1995) 7860.
[25] V.A. de la Peña O'Shea, M.C. Alvarez-Galvan, J.M. Campos-Martin, J.L.G. Fierro, Catal. Comm. (in press).
[26] R. Riva, H. Miessner, R. Vitali and G. Del Piero, Appl. Catal. A 196 (2000) 111.
[27] V.A. Peña O'Shea, N.N. Menéndez, J.D. Tornero and J.L.G. Fierro, Catal. Lett. 88 (2003) 123.
[28] K.S.W. Sing, D.H. Everett, R.A.W. Harel, L. Moscow, R.A. Pierotti, J. Rouquerol and T. Siemienicwska, Pure Appl. Chem. 57 (1985) 603.
[29] Y. Okamoto, T. Nagata, T. Adachi, T. Imanaka, K. Inamura and T. Takyu, J. Chem. Phys. 95 (1991) 310.
[30] G.J. Haddad and J.G. Goodwin Jr, J. Catal. 157 (1995) 56.
[31] E. Steen, G.S. Sewell, R.A. Makhothe, H. Micklethwaite, H. Manstein, M. Lange and C.T. O'Connor, J. Catal. 162 (1996) 220.
[32] A. Sexton, A.E. Hughes and T.W. Turney, J. Catal. 97 (1986) 390.
[33] C.H. Bartholomew, Catal. Lett. 7 (1990) 303.
[34] B.B. Breman, A.A.C.M. Beenackers, E.W.J. Rietjens and R.J.H. Stege, J. Chem. Eng. Data 39 (1994) 647.
[35] H. Pichler, in: *Advances in Catalysis*, W. Frankenburg *et al.* (eds),Vol. IV (Acadamic press, New York, 1952).